Thermorefractive noise reduction of photonic molecule frequency combs using an all-optical servo loop

N.B. When citing this work, cite the original published paper.

(article starts on next page)

Check for updates

Thermorefractive noise reduction of photonic molecule frequency combs using an all-optical servo loop

J. Connor Skehan,[1,†] Anamika Nair Karunakaran,[2,3,†] Poul Varming,[3] Óskar B. Helgason,[1] Patrick B. Montague,[3] Jochen Schröder,[1] Minhao Pu,[2] Kresten Yvind,[2] Victor Torres-Company,[1] and Peter A. Andrekson[1,*]

[1] *Photonics Laboratory, Department of Microtechnology and Nanoscience, Chalmers University of Technology, SE - 412 96 Gothenburg, Sweden*
[2] *Department of Electrical and Photonics Engineering, Technical University of Denmark, Ørsteds Plads 343, DK-2800 Kgs. Lyngby, Denmark*
[3] *NKT Photonics A/S, Blokken 84, DK-3460 Birkerød, Denmark*
[†] These authors contributed equally to this work.
[*] *Peter.Andrekson@Chalmers.SE*

Abstract: Phase and frequency noise originating from thermal fluctuations is commonly a limiting factor in integrated photonic cavities. To reduce this noise, one may drive a secondary "servo/cooling" laser into the blue side of a cavity resonance. Temperature fluctuations which shift the resonance will then change the amount of servo/cooling laser power absorbed by the device as the laser moves relatively out of or into the resonance, and thereby effectively compensate for the fluctuation. In this paper, we use a low noise laser to demonstrate this principle for the first time in a frequency comb generated from a normal dispersion photonic molecule micro-resonator. Significantly, this configuration can be used with the servo/cooling laser power above the usual nonlinearity threshold since resonances with normal dispersion are available. We report a 50 % reduction in frequency noise of the comb lines in the frequency range of 10 kHz to 1 MHz and investigate the effect of the secondary servo/cooling noise on the comb.

1. Introduction

Normal dispersion photonic molecules have recently emerged as one potential solution for the development of high-efficiency, flat-top, and compact optical frequency combs [1,2]. In such a device, an on-chip photonic waveguide is coupled to a normal dispersion ring resonator which, in turn, is coupled to an auxiliary normal dispersion cavity. The coupling between the two resonators induces in an avoided mode-crossing providing localized anomalous dispersion [1,3–11]. Under the right conditions of input power, local dispersion, and pump-to-main-cavity detuning, a photonic molecule may generate a soliton frequency comb which circulates in the main cavity.

The generated frequency comb consists of a series of equally spaced and mutually coherent optical tones which share a common frequency offset from zero [12,13]. In the time domain, this is equivalent to a pulsed output where the repetition rate of the pulses corresponds to the frequency spacing between optical modes, and where the offset frequency between the envelope and carrier waves corresponds to the frequency offset from zero shared between all modes [1].

One of the key parameters of an optical frequency comb that is relevant to applications such as optical communications [14,15], dual comb spectroscopy [16–18], and the generation of tuneable ultra-low-noise sources [19,20] is the phase and frequency noise of individual comb teeth. It is

well understood that that thermal fluctuations are often the driving force behind the majority of noise native to the micro-resonator in integrated comb sources [21–24], and many approaches to reduce or compensate for these thermal effects have been explored, including electrical feedback on the pump [25,26], exploiting dispersive properties of the material itself [27], placing the device directly into a cryostat [28], the application of new coating materials [29], and locking to an OPO [30].

One quite promising approach to reduce phase and frequency noise in micro-resonators makes use of a secondary laser driven into the blue edge of a cavity resonance [3,21,31–33]. This creates a negative feedback loop on temperature of the photonic cavity as a temperature increase (decrease) will cause the resonances to redshift (blueshift) thereby decreasing (increasing) the cavity's absorption of the secondary laser. This negative feedback results in a "cooling" of the device from the perspective of thermorefractive noise, leading to the secondary laser typically being referred to as the cooling laser. Since the actual effect of this laser is to preheat the cavity and provide a fast-acting negative feedback, we prefer to call this the servo laser, and for clarity, use both terms in this publication.

Previous research covering only anomalous dispersion devices has shown a major limitation that can be overcome with photonic molecule micro-resonators [21]. In this key prior art, the pump power of the cooling/servo laser is limited by the threshold for nonlinearity since both the pump and cooling/servo laser are applied to a resonance with anomalous dispersion. Conversely, in a normal dispersion photonic molecule micro-resonator, solitons are initiated by pumping into a resonance with localized anomalous dispersion induced by an avoided mode-crossing of the coupled cavities [2]. This means most other resonances possess normal dispersion and the cooling/servo laser can be applied at significantly higher power without initiating unwanted nonlinearities. Since the cooling/servo and pump resonances share the same spatial mode, the thermal compensation effect is still present when the cooling/servo laser is moved to another resonance in the same mode family [3].

Additionally, this prior art also noted the transfer of noise from the servo/cooling laser onto the cavity and therefor comb as one limiting factor of system performance. We therefore use both a low noise pump and cooling/servo laser to minimize both the initial noise on comb modes, and the noise written onto the cavity (and therefor comb) by the secondary laser. Given the importance of this limitation, we characterize the effects of noise transfer thoroughly, and provide results that serve to inform the choice of servo/cooling laser in future works.

In order to create the lowest noise comb tones possible, we employ a normal dispersion photonic molecule pumped by an ultra-low noise fiber laser and apply a powerful secondary cooling/servo laser to produce a 50 % reduction in frequency noise for the comb lines in the frequency range of 10kHz to 1MHz. To our knowledge, this approach has never been applied to a normal dispersion cavity capable of soliton generation, or to a system of coupled cavities capable of soliton generation. Furthermore, we investigate the role of the cooling/servo laser's noise performance as a limiting factor by modulating tones on to the cooling/servo laser and observing their appearance in the phase noise measurements of comb lines. We report a nearly linear transfer function across the 10 modes measured.

2. Methods

The general schematics for the experiment are given in Fig 1 (a), where a low noise fiber laser (NKT E15 at 1550 nm) pumps the system in the forward direction, while a low noise cooling/servo laser (NKT E15 at 1540 nm) pumps the system in the backwards direction. Phase noise measurements are made at the output, where a tuneable optical filter (TOF) with a 0.1 nm flat-top bandwidth picks off a single optical tone which is amplified using a forward-pumped EDFA (erbium doped fiber amplifier) with approximately 30 dB gain. The single amplified tone is then sent through a tuneable bandpass filter to minimise the appearance of EDFA-related

ASE (amplified spontaneous emission) as phase noise in the measurements. For the modes measured, ASE therefore contributes negligibly. A DC-voltage controlled micro-heater on the auxiliary ring is used to thermal tune the wavelength of the auxiliary resonances. A nearby resonance is tuned close to the primary cavity resonance at our 1550 nm pump wavelength to induce an avoided mode-crossing and generate the necessary localized anomalous dispersion for modulation instability [2]. Although not pictured here, the temperature of the full chip is actively stabilized using a Peltier and TEC attached to the packaged device.
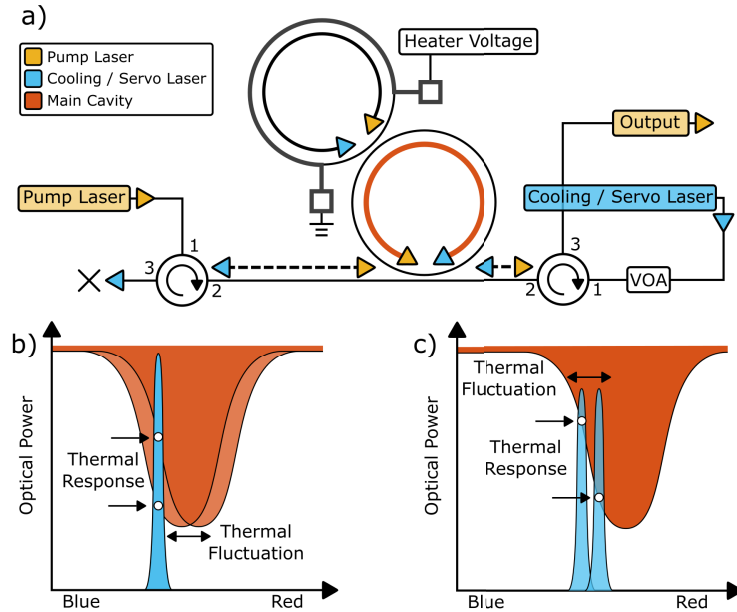
Fig. 1. a) The optical setup, including both the pump and servo/cooling lasers, two circulators, a packaged photonic molecule device with integrated heater only on the auxiliary ring, and a variable optical attenuator to tune the servo/cooling laser power. All fibers are single-mode. b) The principle of action for laser cooling of the main cavity using a backwards pumped, blue detuned servo laser which is assumed to be stationary in the presence of a cavity which experiences temperature fluctuations. As the cavity fluctuates in temperature, the light absorbed by the resonance will fluctuate in response, passively compensating for thermorefractive noise if the servo/cooling laser is placed on the blue side of the optical resonance. c) The principle of action for cavity modulation using a servo laser which fluctuates in frequency, here, a shift in laser frequency will change the amount of light absorbed by the cavity, effectively writing the fluctuation, noise, or modulation onto the cavity.

The micro-resonator device used in the experiment is a Silicon Nitride dual-ring structure fabricated at Chalmers University. It comes from the same production run as the device reported in [2], where the rings have a height and width of 600 nm and 1600 nm, respectively. The ring radii (and FSR [free spectral range]) of the main ring is 217 microns (104 GHz) and for the secondary ring is 213 microns (106 GHz), with the two being separated by 550 nm, and the main ring to bus waveguide gap being 450 nm. The chosen resonances for the pump and cooling/servo wavelength exhibit a quality factor of $3.0 \cdot 10^6$ at 1550 nm and $3.8 \cdot 10^6$ at 1540 nm, respectively. The device is packaged with butt-coupled PM-fiber that has throughput of approximately -10 dB in both directions and requires an input power of 20.5 dBm on the pump laser to produce stable solitons. The parametric threshold for nonlinear processes at the 1550 nm resonance is 16 dBm, which we note is significantly below the cooling/servo laser power

of 20 dBm used in this experiment. Given the similar quality factors of the resonances used by the pump and the cooling/servo laser, the advantage of operating the cooling/servo laser on a normally dispersive resonance is well-demonstrated. We note that applying the cooling/servo laser observably generates no nonlinear effects.

The operating principles of an all-optical servo loop are seen in Figs. 1(b) and (c), where a backwards pumped low noise servo laser sits on the blue side of the optical resonance. Assuming a stable laser and a noisy cavity, a reduction (or increase) in cavity temperature induces a resonance blue (red) shift, thereby causing more (less) absorption of the cooling/servo laser and counteracting the fluctuation in a negative feedback loop. Similarly, if we assume a stable cavity and consider a fluctuating servo laser, it should be clear that both the absorption of light and thus temperature of the cavity will increase as the laser shifts red, and decrease as the laser shifts blue, thereby writing the laser's frequency fluctuations onto the cavity. The first set of assumptions is used to study thermorefractive noise reduction, while the second set of assumptions is used for recovery of the transfer function of noise from the servo laser onto the output comb line, as explored later in this paper. We note for clarity that the servo laser wavelength is fixed at all times and that servo actuation refers to the negative feedback effect that this variable absorbed power has on the micro-resonator temperature.

The shift in resonant frequency, $\Delta\omega$, for a whispering gallery mode resonator as a function of temperature, T, is given by

$$\frac{\Delta\omega}{\omega} = -\left(\frac{1}{n}\frac{\partial n}{\partial T} + \alpha_T\right)\Delta T, \tag{1}$$

which includes the change due to a difference in the refractive index, n, and the coefficient of thermal expansion, α_T [34].

Importantly, if a $\Delta\omega$ fluctuation is so large that the cooling/servo laser is moved onto the red side of the resonance, the servo effect will be reversed to provide a positive feedback i.e. an increase in temperature will instead cause a blue shift that gives greater absorption. In practice, the servo laser being on the red side of the resonance should result in a short period of increased amplified thermorefractive noise and then the quick loss of the soliton state, due to the sudden change in cavity-to-pump detuning.

It is also important, for the sake of comparison between measurements, to keep the offset between the resonance and servo/cooling laser stable. In our case, we keep the servo laser approximately halfway into the resonance and maintain this position by carefully monitoring the transmission trace of the servo/cooling laser on an oscilloscope and adjusting laser frequency accordingly.

As shown in Fig. 2 (a), we apply a triangular voltage ramp to the piezo controller of the pump laser. This induces a triangular sweep in the laser frequency spanning 8 GHz (64 pm), where an increase in piezo voltage corresponds to a decrease in frequency. We then record the transmission of pump and servo/cooling laser through the micro-resonator, using a photodiode and an oscilloscope. Sweeping from blue-to-red across the main resonance with the servo/cooling laser off, we observe a characteristic "thermal triangle" in the transmission of pump resonance [35,36]. This arises when the increased laser absorption heats up the cavity and red shifts the resonance, as expressed by Eq. (1). As such, a red sweeping laser will push the resonance along with it to create a region of thermal bistability until the laser wavelength surpasses the cavity red-shifting and the resonance abruptly recoils to its original wavelength, resulting in a steep transition of the transmission to zero.

Conversely, when a cooling/servo laser is applied at high power, the cavity is pre-heated and red-shifting of the cavity induced by the pump laser is compensated for by a drop in heat absorption from the cooling/servo laser as it moves up the blue slope of the resonance. In Fig. 2 (a), we see this in the narrowing of the thermal triangle for the cooled pump laser transmission in comparison to the uncooled transmission; this more closely resembling a Lorentzian line
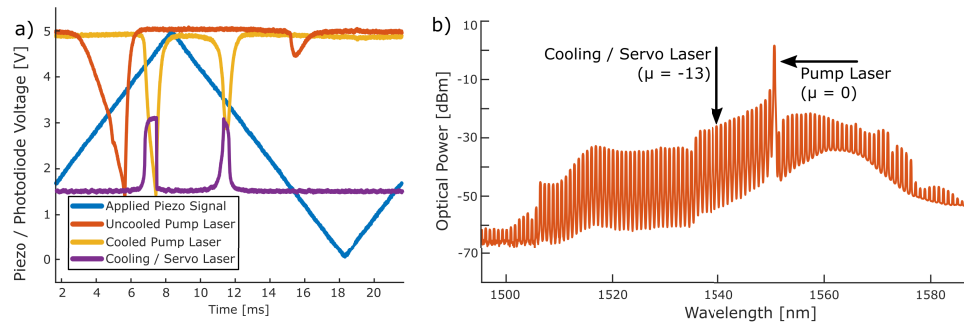
Fig. 2. a) Oscilloscope traces of the applied piezo signal used to tune the pump laser wavelength (blue), the uncooled pump laser photodiode voltage after transmission through the device (orange), and finally, the photodiode voltage after transmission in the case of passive cooling for both the pump (yellow) and servo/cooling (purple) lasers. NB: An increase in piezo voltage corresponds to a decrease in frequency. b) The optical spectrum of the generated frequency comb, with resonances corresponding to the pump laser ($\mu = 0$) at 1550 nm and servo/cooling laser ($\mu = -13$) at 1540 nm labeled.

shape in comparison to the thermal triangle of the uncooled transmission. We can also notice the pre-heating of the cavity in the presence of the cooling/servo laser, which appears as a fixed offset (red-shift) between the cooled and uncooled transmission dips. Additional insight to these dynamics is shown in the purple trace of Fig. 2 (a) (cooling/servo laser transmission), which shows the initially low transmission increases as we sweep the pump laser across the main cavity resonance. The cooling/servo laser, which begins on the blue-side slope of the cooling resonance, moves out of the resonance as the pump laser moves into the pump resonance, thereby limiting cavity temperature shift. Importantly, in Fig. 2 (a), we see that the effect of thermal dragging on the uncooled transmission is asymmetric and depends strongly on the direction of sweep. However, when cooled, the resonance dips become quite symmetric regardless of the direction of sweep, providing direct evidence that the effect corrects for fluctuations which either heat or cool the system.

Generation of frequency combs in normal dispersion micro-resonators requires localised anomalous dispersion close to the pump resonance. In the photonic molecule device, the localised anomalous dispersion is attained by coupling the modes of the main ring and the auxiliary ring. In our experiment, the mode coupling is tuned by changing the voltage applied to the heater on the auxiliary ring. Once the mode coupling is tuned close to the pump resonance, the pump laser is moved into the resonance from the blue side until we observe the generation of Turing rolls due to nonlinear effects in the cavity. The mode coupling is further tuned (via the voltage on the heater of auxiliary ring) to generate the stable soliton states from this device. We verify the presence and stability of this soliton state by measuring the RF noise of the converted power trace on an electrical spectrum analyser, observing it equal to the noise floor for the measurement range of 0-150 MHz. We also note that this spectrum is typical of a dark soliton comb [2]. In order to "cool" the soliton, the servo laser is then tuned into the corresponding resonance until it is halfway in the blue side, while minor adjustments are made to the pump detuning and heater to maintain soliton operation. The optical spectrum of the cooled soliton shown in Fig. 2 (b), corresponds well with models of the spectral envelope predicted for a photonic molecule soliton frequency comb, and is notably different from the sech^2 spectral envelope seen in anomalous dispersion single resonator microcombs. The dynamics of mode splitting also match well with predictions from theory [2].

The frequency noise measurements in this work are carried out using a homodyne interferometer system, isolated from environmental noise by being placed in a vacuum chamber, which itself sits inside a vibration isolating container made from polystyrene. The interferometer has an unbalanced arm of 20 m, which corresponds to an oscillation frequency of 5 MHz. By measuring the amplitude of the sinusoidal output of the photodiode, and knowing the fixed frequency of oscillation, the measured optical power fluctuations can be converted into the frequency fluctuations of the optical signal. This assumes that the recovered trace remains within a narrow range around the quadrature point such that we may make a linear approximation of the sine wave. The system is very accurate for low noise signals, and produces nearly identical results to commercial setups without limitation on the noise floor. Conversely, it does have a limited ceiling, given that large fluctuations will push the trace away from the quadrature point. It is thus unsuitable to measure comb tones very far from the pump, where thermorefractive noise increases the phase noise of the comb lines beyond the range of the measurement tool.

3. Results and discussion

Raw traces of the uncooled and cooled comb modes $\mu = 0$ to $\mu = -10$ are shown in Figs. 3(a) and (b) respectively, along with the linear case of the amplified pump passing through the device in the absence of a soliton. Here, we use a planar cavity operating with a single spatial mode such that the mode number $\mu = 0$ corresponds to the comb mode at the pump wavelength, and $\mu = -13$ to the mode used for laser cooling of the device.

Noise in the low frequency regime remains largely unchanged between comb modes and is unaffected by cooling. In the acoustic range (~ 2.5 kHz), however, we see a difference in phase noise between the cooled and uncooled soliton. Here, noise increases as a function of comb mode index for both, but more significantly increases for the cooled case. This suggests acoustic and mechanical vibrations which are picked up by both the pump and servo laser dominate the noise in this frequency range. The increase in measured noise for the cooled case is likely due to the servo/cooling laser "writing" this added noise onto the cavity. We note that measurements are limited to 2.5 MHz, due to observed resonant interaction with the interferometer at 5 MHz.

In the portion of the spectrum dominated by thermorefractive noise ($10^4 - 10^6$ Hz), the phase and frequency noise for all modes is significantly lower when the soliton is cooled via servo back-action. This is investigated further in Fig. 3 (c) by isolating the $\mu = -10$ modes for the cooled and uncooled state and comparing it to the pump laser before passing through the cavity. We take note of the nearly white noise across this region, which appears across this frequency range for all comb modes in the uncooled and cooled states, and plot the average in Fig. 3 (d). Over all modes measured, the servo/cooling laser results in an approximately 50 % reduction in noise across the thermorefractive-noise dominated region (in Hz/$\sqrt{\text{Hz}}$).

In order to better understand this process, we simulate strong noise at a specific frequency by applying a modulation tone at 50 kHz to the servo laser. In Fig. 4, we demonstrate that this modulation tone is only written onto the comb modes when the laser is positioned within the cavity (which in this case, simultaneously cools the device), and when modulation is turned on. The strength of the recovered tone is given for each of 10 comb modes in the right panel of the same Fig., demonstrating an approximately linear increase of noise as a function of absolute mode index, reinforcing the primary result of Fig. 3 and validating that such a method may be used to track comb mode noise at different frequencies and at high modulation intensities. Moreover, it demonstrates that modulation tones from a cooling laser may be directly written onto a cavity and shared between all comb modes.

Finally, in Fig. 5 (a), we broaden this investigation by applying modulation tones at frequencies ranging from 10 to 70 kHz to the servo laser and directly recover the frequency noise component at the frequency of modulation without passing through the device. We then reduce the modulation level by a factor of 4, generate a cooled soliton in the modulated cavity, and recover the transfer
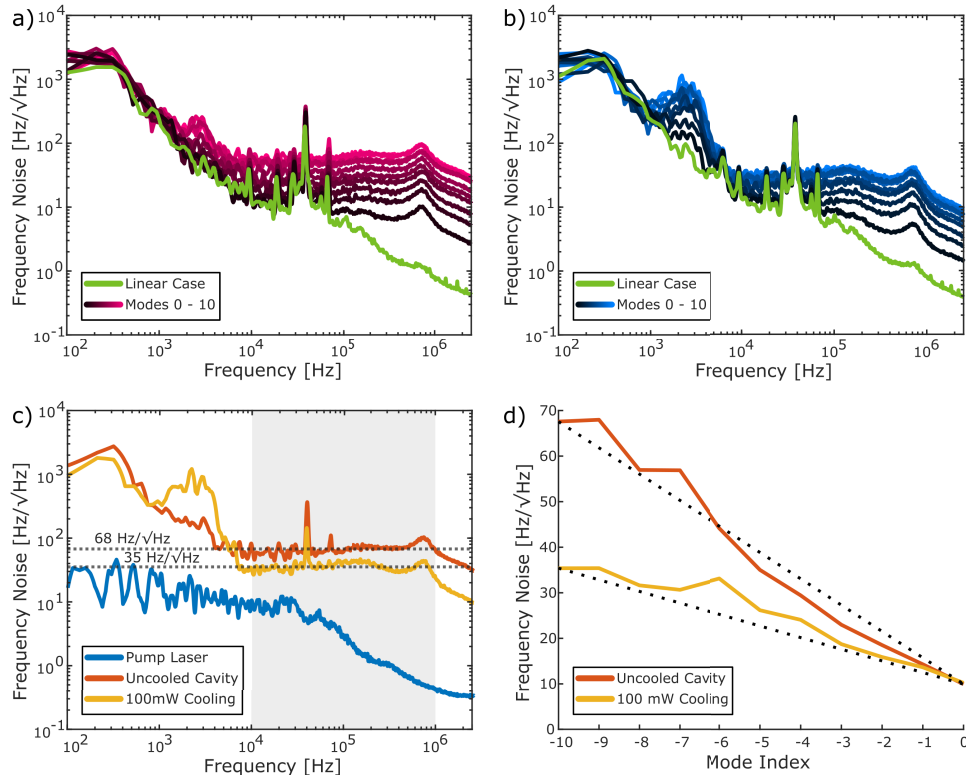
Fig. 3. a) The frequency noise spectrum for the cases of linear transmission (such that nonlinear effects are negligible) of the amplified pump (green) and the uncooled (magenta) soliton modes $\mu = 0$ to -10. b) The frequency noise spectrum for the cases of linear transmission of the amplified pump (green) and the cooled (blue) soliton modes $\mu = 0$ to -10. c) The frequency noise spectra of the non-amplified pump laser (blue) without passing through the cavity, as well as of the uncooled (orange) and cooled (yellow) $\mu = -10$ comb modes. The grey box indicates the region of thermorefractive noise in question (10-1000 kHz). d) The average frequency noise across the thermorefractive regime for the uncooled (orange) and cooled (yellow) cases, for modes $\mu = 0$ to $\mu = -10$, along with a linear approximation of noise growth as a function of mode index.

function (i.e. the modulation tone) from the $\mu = 3$ comb mode by repeating measurements at the same modulation frequencies as before. The modulation level does not have units and is related to an internal driving voltage within the pump laser. This allows us to construct a multiplication factor for each frequency, seen in Fig. 5 (b), suggesting a nearly linear transfer function of noise from the servo laser onto the comb modes. However, to construct this transfer function, we require a scaling factor, given that the internal modulation strength for the two measurements in the left panel are different. This scaling factor is shown in Fig. 5 (c) to be linear over a wide range of modulation strengths, and allows us to use the modulation level as an analog for frequency noise in terms of Hz/$\sqrt{\text{Hz}}$. The recovered multiplication factor for mode $\mu = 3$ is $\approx 0.8 \pm 0.2$, which indicates that a 1000 Hz/$\sqrt{\text{Hz}}$ tone on the servo laser will produce a tone at the same modulation frequency (but different optical frequency), with strength approximately 800 Hz/$\sqrt{\text{Hz}}$. We assume that the linearity of the transfer function holds true for all mode numbers.
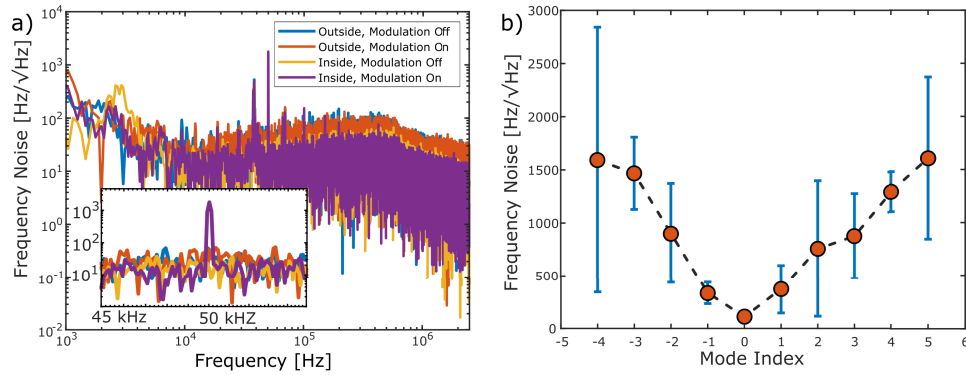
Fig. 4. a) A comparison of the 4 main cases for a modulated servo laser, for the $\mu = 3$ comb mode, including when the servo laser is outside the resonance, and unmodulated (blue), when the servo laser is outside the resonance and modulated at 50 kHz (orange), when the servo laser is inside the resonance but not modulated (yellow), and when the servo laser is inside the resonance and modulated at 50 kHz. As highlighted in the inset, the modulation tone at 50 kHz from the cooling laser is only transferred onto comb modes when inside the resonance, and is done so while simultaneously reducing thermorefractive noise in the main ring. b) Recovered frequency noise at 50 kHz for each of 10 comb modes, $\mu = -4$ to 5. Error bars represent the standard deviation of 5 measurements, and become significant due to limitations native to the homodyne interferometer.
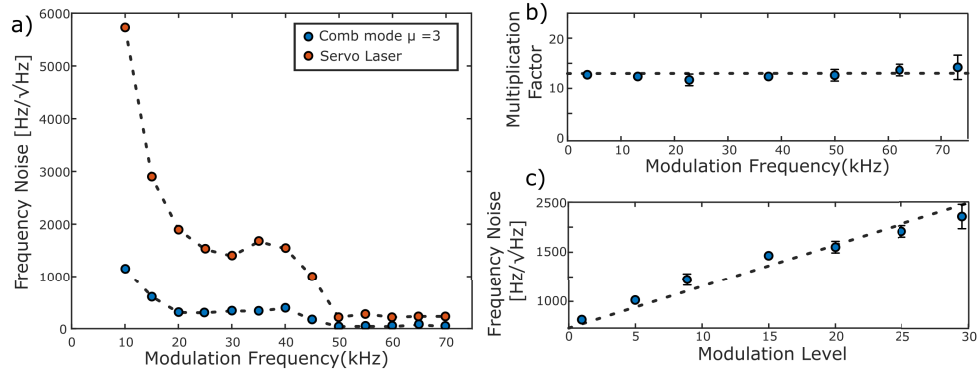
Fig. 5. a) Recovered frequency noise as a function of modulation frequency for the $\mu = 3$ comb mode (blue) and for the servo laser without passing through the chip (orange). b) The multiplication factor which relates the modulation strength on the servo laser to the modulation strength of the $\mu = 3$ tone, as a function of modulation frequency, indicating a nearly linear transfer function of noise on the servo laser to comb modes. c) the frequency noise of the servo as a function of modulation level, measured without passing through the device, used to calculate the multiplication factor above.

4. Conclusion and future outlook

In conclusion, we have successfully demonstrated laser cooling of a photonic molecule micro-comb consisting of two coupled normal-dispersion resonators. Previous studies on thermorefractive noise reduction in anomalous dispersion micro-resonators identified two key limiting factors in system performance, both of which are addressed here. Using a set of normal dispersion micro-resonators, and relying on their avoided mode-crossing, we generate solitons in resonances with localized anomalous dispersion. This allows, for the first time, demonstration of the

cooling/servo effect using a secondary laser driven into an offset mode with normal dispersion. In normal dispersion, the laser does not fulfil the conditions for parametric nonlinearity (in particular modulation instability), and could therefore be driven at higher power (20 dBm) than previously studied. The cooling/servo effect in our system resulted in an approximately 50% reduction in frequency noise amplitude (in Hz/$\sqrt{\text{Hz}}$) over the full thermorefractive bandwidth (10 kHz – 1 MHz). This is significant for systems whose performance is limited by frequency noise in this range as it effectively doubles their useable optical bandwidth, and may be useful for optical metrology, communications, and the generation of broadband tunable lasers, among others.

We also studied the mechanism of noise transfer from the cooling/servo laser onto the comb modes by modulating the cooling/servo laser at various strengths and frequencies and measuring the output frequency noise on the comb modes. This validates previous reports showing that noise on the cooling/servo laser can be a limiting factor on the noise reduction effect. In our experiment, we observed an amplification factor of 0.8 on mode $\mu = 3$, meaning, for instance, a frequency noise level of 1000 Hz/$\sqrt{\text{Hz}}$ from the servo/cooling laser limits the frequency noise of mode $\mu = 3$ to a minimum of 800/$\sqrt{\text{Hz}}$. It is currently unclear if the servo laser, control electronics, or effective loop length limit system performance. This investigation justifies the use of an ultra-low noise laser for both the pump and servo/cooling lasers along with a set normal dispersion coupled cavities in order to produce the lowest noise comb tones possible.

Disclosures. The authors declare no conflicts of interest.

JCS designed and proposed the study, while ANK and JCS performed experiments together. The paper itself was written by JCS. PV assisted with the EDFA, homodyne interferometer and phase noise measurement. PBM served as the day-to-day supervisor of experiments. JS, MP, KY, VTC, and PAA served as principle and co-supervisors for the experiment.

Data availability. Data underlying the results presented in this paper are not publicly available at this time but may be obtained from the authors upon reasonable request.

References

1. X. Xue, Y. Xuan, P.-H. Wang, Y. Liu, D. E. Leaird, M. Qi, and A. M. Weiner, "Normal-dispersion microcombs enabled by controllable mode interactions," Laser Photonics Rev. **9**(4), L23–L28 (2015).
2. Ó. B. Helgason, F. R. Arteaga-Sierra, Z. Ye, K. Twayana, P. A. Andrekson, M. Karlsson, J. Schröder, and V. Torres-Company, "Dissipative solitons in photonic molecules," Nat. Photonics **15**(4), 305–310 (2021).
3. X. Sun, R. Luo, X.-C. Zhang, and Q. Lin, "Squeezing the fundamental temperature fluctuations of a high-q microresonator," Phys. Rev. A **95**(2), 023822 (2017).
4. D. D. Smith, H. Chang, and K. A. Fuller, "Whispering-gallery mode splitting in coupled microresonators," J. Opt. Soc. Am. B **20**(9), 1967–1974 (2003).
5. A. Tikan, J. Riemensberger, and K. Komagata, *et al.*, "Emergent nonlinear phenomena in a driven dissipative photonic dimer," Nat. Phys. **17**(5), 604–610 (2021).
6. S. Fujii, Y. Okabe, R. Suzuki, T. Kato, A. Hori, Y. Honda, and T. Tanabe, "Analysis of mode coupling assisted Kerr comb generation in normal dispersion system," IEEE Photonics J. **10**(5), 1–11 (2018).
7. C. Schmidt, M. Liebsch, and A. Klein, *et al.*, "Near-field mapping of optical eigenstates in coupled disk microresonators," Phys. Rev. A **85**(3), 033827 (2012).
8. Y. Liu, Y. Xuan, X. Xue, P.-H. Wang, S. Chen, A. J. Metcalf, J. Wang, D. E. Leaird, M. Qi, and A. M. Weiner, "Investigation of mode coupling in normal-dispersion silicon nitride microresonators for Kerr frequency comb generation," Optica **1**(3), 137–144 (2014).
9. X. Xue, M. Qi, and A. M. Weiner, "Normal-dispersion microresonator Kerr frequency combs," Nanophotonics **5**(2), 244–262 (2016).
10. J. K. Jang, Y. Okawachi, M. Yu, K. Luke, X. Ji, M. Lipson, and A. L. Gaeta, "Dynamics of mode-coupling-induced microresonator frequency combs in normal dispersion," Opt. Express **24**(25), 28794–28803 (2016).
11. Y. Zhang, M. Menotti, K. Tan, V. Vaidya, D. Mahler, L. Helt, L. Zatti, M. Liscidini, B. Morrison, and Z. Vernon, "Squeezed light from a nanophotonic molecule," Nat. Commun. **12**(1), 1–6 (2021).
12. T. Fortier and E. Baumann, "20 years of developments in optical frequency comb technology and applications," Commun. Phys. **2**(1), 153 (2019).
13. L. Chang, S. Liu, and J. E. Bowers, "Integrated optical frequency comb technologies," Nat. Photonics **16**(2), 95–108 (2022).

14. M. Tan, B. Corcoran, and X. Xu, *et al.*, "Optical data transmission at 44 terabits/s with a Kerr soliton crystal microcomb," Proc. SPIE **11713**, 117130C (2021).

15. B. Corcoran, M. Tan, and X. Xu, *et al.*, "Ultra-dense optical data transmission over standard fibre with a single chip source," Nat. Commun. **11**(1), 2568 (2020).

16. I. Coddington, N. Newbury, and W. Swann, "Dual-comb spectroscopy," Optica **3**(4), 414–426 (2016).

17. N. R. Newbury, I. Coddington, and W. Swann, "Sensitivity of coherent dual-comb spectroscopy," Opt. Express **18**(8), 7929–7945 (2010).

18. M.-G. Suh, Q.-F. Yang, K. Y. Yang, X. Yi, and K. J. Vahala, "Microresonator soliton dual-comb spectroscopy," Science **354**(6312), 600–603 (2016).

19. J. C. Skehan, C. Naveau, J. Schroder, and P. Andrekson, "Widely tunable, low linewidth, and high power laser source using an electro-optic comb and injection-locked slave laser array," Opt. Express **29**(11), 17077–17086 (2021).

20. J. C. Skehan, Ó. B. Helgason, and J. Schröder, *et al.*, "Widely tunable narrow linewidth laser source based on photonic molecule microcombs and optical injection locking," Opt. Express **30**(13), 22388–22395 (2022).

21. T. E. Drake, J. R. Stone, T. C. Briles, and S. B. Papp, "Thermal decoherence and laser cooling of Kerr microresonator solitons," Nat. Photonics **14**(8), 480–485 (2020).

22. F. Lei, Z. Ye, Ó. B. Helgason, A. Fülöp, M. Girardi, and V. Torres-Company, "Optical linewidth of soliton microcombs," Nat. Commun. **13**(1), 1–9 (2022).

23. A. B. Matsko, A. A. Savchenkov, N. Yu, and L. Maleki, "Whispering-gallery-mode resonators as frequency references. i. fundamental limitations," J. Opt. Soc. Am. B **24**(6), 1324–1335 (2007).

24. A. A. Savchenkov, A. B. Matsko, V. S. Ilchenko, N. Yu, and L. Maleki, "Whispering-gallery-mode resonators as frequency references. ii. stabilization," J. Opt. Soc. Am. B **24**(12), 2988–2997 (2007).

25. P. Del'Haye, A. Coillet, T. Fortier, K. Beha, D. C. Cole, K. Y. Yang, H. Lee, K. J. Vahala, S. B. Papp, and S. A. Diddams, "Phase-coherent microwave-to-optical link with a self-referenced microcomb," Nat. Photonics **10**(8), 516–520 (2016).

26. P. Del'Haye, S. B. Papp, and S. A. Diddams, "Hybrid electro-optically modulated microcombs," Phys. Rev. Lett. **109**(26), 263901 (2012).

27. J. R. Stone and S. B. Papp, "Harnessing dispersion in soliton microcombs to mitigate thermal noise," Phys. Rev. Lett. **125**(15), 153901 (2020).

28. G. Moille, X. Lu, A. Rao, Q. Li, D. A. Westly, L. Ranzani, S. B. Papp, M. Soltani, and K. Srinivasan, "Kerr-microresonator soliton frequency combs at cryogenic temperatures," Phys. Rev. Appl. **12**(3), 034057 (2019).

29. J. Lim, A. A. Savchenkov, E. Dale, W. Liang, D. Eliyahu, V. Ilchenko, A. B. Matsko, L. Maleki, and C. W. Wong, "Chasing the thermodynamical noise limit in whispering-gallery-mode resonators for ultrastable laser frequency stabilization," Nat. Commun. **8**(1), 1–7 (2017).

30. J. K. Jang, Y. Zhao, Y. Okawachi, X. Ji, M. Lipson, and A. L. Gaeta, "Phase noise reduction of a Kerr comb via all-optical synchronization to an optical parametric oscillator," in *2022 Conference on Lasers and Electro-Optics (CLEO)*, (IEEE, 2022), pp. 1–2.

31. F. Lei, Z. Ye, and V. Torres-Company, *et al.*, "Thermal noise reduction in soliton microcombs via laser self-cooling," Opt. Lett. **47**(3), 513–516 (2022).

32. J. Jost, E. Lucas, T. Herr, C. Lecaplain, V. Brasch, M. Pfeiffer, and T. Kippenberg, "All-optical stabilization of a soliton frequency comb in a crystalline microresonator," Opt. Lett. **40**(20), 4723–4726 (2015).

33. K. Nishimoto, K. Minoshima, T. Yasui, and N. Kuse, "Thermal control of a Kerr microresonator soliton comb via an optical sideband," Opt. Lett. **47**(2), 281–284 (2022).

34. I. Grudinin, H. Lee, T. Chen, and K. Vahala, "Compensation of thermal nonlinearity effect in optical resonators," Opt. Express **19**(8), 7365–7372 (2011).

35. T. Carmon, L. Yang, and K. J. Vahala, "Dynamical thermal behavior and thermal self-stability of microcavities," Opt. Express **12**(20), 4742–4750 (2004).

36. X. Jiang and L. Yang, "Optothermal dynamics in whispering-gallery microresonators," Light: Sci. Appl. **9**(1), 1–15 (2020).